

Model studies of V^0 production ratios in pp collisions at $\sqrt{s} = 0.2, 0.9$, and 7 TeV

M. Ajaz^{1*}, M.U. Ashraf², M. Waqas^{3†}, Z. Yasin⁴, S. Hassan⁴, M. K. Suleymanov⁵

¹ Department of Physics, Abdul Wali Khan University Mardan, 23200 Mardan, Pakistan,

² National Center for Physics, Shahdra Valley Road, Islamabad 44000, Pakistan

³ School of Nuclear Science and Technology, University of Chinese Academy of Sciences, Beijing 100049, China

⁴ Pakistan Institute of Nuclear Science and Technology (PINSTECH), Islamabad 44000, Pakistan

⁵ Baku State University, Baku Azerbaijan

Abstract

A comparative study of V^0 ratios has been performed between HIJING, Sibyll and QGSJET model-based event generators in this paper. The ratios under study are $\bar{\Lambda}/\Lambda$, $\bar{\Lambda}/K_S^0$ and Ξ^-/Λ as a function of rapidity y , rapidity loss (Δy) and p_T from pp collisions at $\sqrt{s} = 0.2, 0.9$, and 7 TeV and these simulations are then compared with the STAR and LHCb fiducial phase spaces in different p_T regions. Although the models could produce some of the ratios in a limited p_T and/or y region, none of them completely predicts the experimental results. The QGSJET has good predictions with the data in most of the cases but since the model does not include the Ξ particle definition, therefore it does not give any predictions for Ξ/Λ ratios. The extrapolation to the highest possible energies can be studied by re-tune some of the basic parameters based on current and previous measurements. These kinds of systematic comparison studies are also useful to apply certain constraints on the pQCD and non-pQCD-based hadronic event generators to significantly improve the predictions of Standard Model physics at the RHIC and LHC experimental data for the understanding of underlying physics mechanisms in high energy collisions.

Keywords— Strange particles, Transverse momentum spectra, Rapidity distribution, Monte Carlo prediction, LHC energies, proton-proton collisions

1 Introduction

A deconfined, strongly interacting state of matter, called Quark-Gluon Plasma (QGP) is conjectured to be produced, at high temperatures and densities, in collisions recorded at high-energy physics experiments. The formation of QGP is gauged with several proposed signatures including production and ratios of strange particles. The transverse momentum (p_T) spectra of strange particles also serve an important role in the determination of freezeout parameters [1–3]. Strange hadrons production in relativistic high energy collisions is an invaluable tool to investigate the properties of collision phases since these are not part of the colliding nuclei from the incoming beams. Strange particles have been studied extensively in high energy particle physics as their production and distribution in phase space provide information on the fireball and properties of the created medium [4]. In the initial stages, after a collision, flavor creation and excitation are mainly responsible for strangeness production at high p_T (gluon splittings dominate in the later evolution). While at low p_T , non-perturbative partonic processes contribute predominantly to the strangeness production [5, 6].

High energy proton-proton (pp) collisions provide a simple system to investigate the structure of nuclear matter and the basic workings of the universe. Many recent developments in fundamental particle physics including the discovery of the Higgs boson proved the importance of pp collision systems. Additionally, pp collision system serves as a baseline guide for the investigations of complex proton-nucleus (pA) and nucleus-nucleus (AB) collision systems. Transverse momentum (p_T) spectra in pp collisions are used as reference in heavy-ion (pA, AB) collisions

*Corresponding author: ajaz@awkum.edu.pk; muhammad.ajaz@cern.ch (M. Ajaz)

†Corresponding author: waqas_phy313@yahoo.com; waqas_phy313@ucas.ac.cn (M. Waqas)

for the studies of initial state effects. The high-energy heavy-ion collisions are important to characterize the quark-gluon plasma (QGP). However, many signatures typical to the heavy-ion collisions have also been observed in high multiplicity pp collisions [7, 8] including recent observation of enhanced production of strange and multi-strange particles [9]. Monte-Carlo's studies of the production of strange and multi-strange particles in pp collisions are thus important to characterize not only the pp systems but can further be extended to compare the production of enhanced strangeness in different collision systems.

Perturbative Quantum-Chromodynamics (pQCD) well describes the particle production at high transverse momentum (p_T) but in the low (p_T) regions, involving predominant soft processes, phenomenological models are commonly employed. Baryon production in this region particularly lacks a full QCD-based description. The ambiguity lies in, whether the baryon number should be associated with the valence quarks of a hadron or with its gluonic field? Phenomenological processes involving (anti-)string junctions and negative C-parity exchanges may give rise to differences between spectra of particles and the corresponding anti-particles. Spectra of (anti-)baryons can provide information regarding competing mechanisms responsible for the baryon production in pp collisions. The anti-baryon to baryon ratio of the hadrons with different valence quark content, at different collision energies is considered one of the most direct methods to constrain the baryon production mechanisms [10]. Particle ratios provide simplification for the comparison of different experiments performed under different trigger and centrality conditions, and systematic errors associated with absolute particle yields are reduced while working with ratios. Strange to non-strange, mixed particle ratios play an important role in the quantitative analysis of strangeness production and serve as crucial probes for strangeness enhancement studies [11]. Particle ratios, such as (p/π) and (Λ/K_S^0) , provide important insights regarding production mechanisms and the spectral shapes, especially in the intermediate transverse momentum region [12]. Confronting the model predictions from phenomenological models with experimental observations provide insights on parameters tuning for further improvements in the models [6]. QGP features and other insights gained from the study of strange particle production ratios may prove to be helpful in parameter tuning of Monte Carlo models.

In this study anti-baryon to baryon ratios are presented vs the strangeness number: $0(\bar{p}/p)$, $1(\bar{\Lambda}/\Lambda)$, $2(\bar{\Xi}/\Xi)$ and $3(\bar{\Omega}/\Omega)$. The ratios $(\bar{\Lambda}/\Lambda)$, $(\bar{\Xi}/\Xi)$ as a function of p_T are calculated with hadronic models and contrasted with the corresponding experimental data. The ratio $(\bar{\Lambda}/\Lambda)$ gives the information on the baryon-number transport between proton-proton pp collision state to the final state hadrons. Furthermore, the ratio (Λ/K_S^0) shows the suppression of baryon to meson ratio in strange quark hadronization [13]. In this paper, the ratios (Λ/K_S^0) are presented as a function of (p_T), Rapidity (y), and Rapidity loss (Δy) in pp collisions at $\sqrt{s} = 200$ GeV, 900GeV and 7.0 TeV as calculated with HIJING, Sibyll2.3d and QGSJETII-04 models. A thorough comparison is made between experimental and simulation results and underlying features giving rise to differences in modelling results are discussed.

Particle production in high energy collisions includes contributions from both the hard processes (explained with perturbative Quantum Chromodynamics, pQCD) and the soft processes that are currently understood with phenomenological models [14, 15]. Confronting predictions from such hadronic models with experimental observations provide insights on parameters tuning for further improvements in the models [6, 16–24].

The paper is organized into four sections: In section 2, the phenomenological models used for the study are described briefly. Section 3 gives results and discussion, and finally, the results are concluded in section 4.

2 Methods and Models

The hadronic models, HIJING, Sibyll2.3d and QGSJETII-04, used in this study are briefly described as under.

HIJING model is a Monte Carlo framework of heavy ions based on the basic structure of C++ and CPU based parallelism. HIJING is designed to observe the production of jets and multi-particles in pp , pA and AA high energy collisions. HIJING has the capability to adjust the parameters for the production of multi-particles in pp collisions, in order to retrieve the essential information of initial conditions in the energy range ($\sqrt{s_{NN}} = 5 - 2000$ GeV) [25]. HIJING, a heavy-ion jet interaction generator, utilizes the LUND model for the fragmentation of jets and the QCD-inspired models for the production of jets. To study the nuclear consequences, the shadowing effect is also

incorporated for the structuring of parton functions [26]. In addition, the model of HIJING includes phenomenology of multi-strings at low p_T interaction, thereby combining the physics of fragmentation at inter-mediate energy with perturbative physics at the energy of collisions [27]. The model also includes the effects of the production of multiple mini jets, soft excitations and jet interactions in hadronic dense matter [26, 28].

The **Sibyll2.3d** model is based on mini-jet modeling with the ability of multiple hard parton interactions per hadron collision. In this model, the effects of energy-momentum conservation drive the change in the distribution of leading particles. In this model of Sibyll multiplicity of average particles is high at higher energy [29]. The basic purpose of the event-generator Sibyll2.3d is to take into account the main characteristics of hadronic-particle production and strong interactions. These characteristics are required for the study of air-shower cascades and fluxes of secondary particles which are produced via the interaction of cosmic rays with the atmosphere of Earth [30]. This model consists of a combination of Gribov Regge theory and QCD perturbative field theory with the inclusion of elastic and total cross-sections for p-p, K-p and π -p interactions in order to retrace the new LHC data [31]. In this version of the Sibyll model, the production of charm-hadrons is also included in the studies of atmospheric neutrinos at high energies. In addition to charm hadrons, the abundance of muons is increased as compared to previous versions to well remove the difference between simulation and data [30]. Sibyll model also describes the excited states' diffractive production of projectiles and targets, leading-particle distributions with different energies and particle production in forward phase-space [31].

QGSJETII-04 is a Monte Carlo event generator based on the Quark-Gluon String model developed for hadronic interactions. The generator of QGSJETII-04 relies on the Quark-Gluon String model, effective field theoretical framework of Gribov-Regge and LUND algorithm to explain the interactions of high-energy particles and to study phenomena of multiple-scattering. For the nucleus-nucleus interactions and semi-hard processes, the QGSJET model employs the “Semi-hard pomerons” approach [31, 32]. The coupling of Pomeron in the QGSJETII-04 model is derived from the framework of Gribov Regge theory. The coupling of pomeron-pomeron represents the cascade of parton interaction when pomerons overlap in phase-space. QGSJETTII-04 event generator requires fewer parameters for a simulation [32] and can incorporate mini jets. The new version of QGJETII-04 is tuned with experimental data from LHC experiments. QGSJETII-04 model reproduces the experimental data at higher-momentum to a good extent, while the particle distributions are over-estimated at lower-momentum [33, 34].

3 Results and discussion

The events have been generated for various strange particles, K_S^0 , $\Lambda(\bar{\Lambda})$ and $\Xi^-\bar{\Xi}^+$ using different models including HIJING, Sibyll and QGSJET at $\sqrt{s} = 0.2, 0.9$, and 7 TeV. The pQCD-based model HIJING and cosmic ray air shower based models Sibyll and QGSJET gives different predictions at all energies. In order to validate the MC simulation results, a detailed comparison has been made with that of experimental results from pp collision at $\sqrt{s} = 200$ GeV from STAR experiment at RHIC [35] and LHCb experiment at $\sqrt{s} = 0.9$ and 7 TeV [36].

For a gluon jet, there exists no leading baryon against anti-baryon, while in the case of a quark jet this expectation is reversed as there exists a leading baryon against anti-baryon. Therefore, the hadron production mechanisms at high p_T are dominated by the jet fragmentation and it is a reasonable expectation that with the increase in p_T the \bar{B}/B ratio will start to decrease. This decreasing trend in \bar{B}/B ratios has been predicted previously [37]. Figures 1a and 1b shows the anti-baryon to baryon ($\bar{\Lambda}/\Lambda$) and $\bar{\Xi}^+/\Xi^-$ ratio as a function of p_T respectively. It has been observed that all models describe the experimental data with reasonable agreement while taking into account the error bars and χ^2/n calculated in each case given in Table 1. Among the three, for both the ratios, the Sibyll gives a better description of data, particularly for the $\bar{\Xi}^+/\Xi^-$ ratio than the other model where the QGSJET did not produce any result. However, large error bars in data, as well as models, makes it difficult to observe the ratios follow decreasing trend at high p_T .

The mean anti-baryon to baryon (\bar{B}/B) ratio as a function of strangeness content from pp collisions at $\sqrt{s} = 200$ GeV from STAR compared with different models can be seen in figure 2. The ratio shows a slightly increasing trend with an increase in strangeness content in the case of the experimental data, while the models show a completely different trend. In the case of the experimental data, for protons and Λ baryons the \bar{B}/B ratio is not unity and

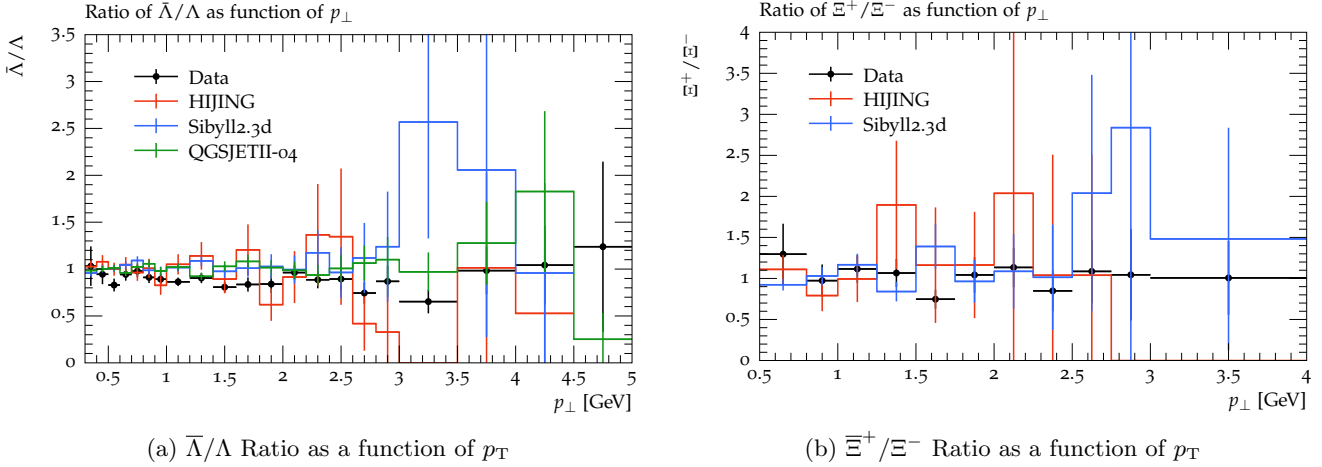


Figure 1: Anti-baryon to baryon ratios as a function of p_T in pp collisions at $\sqrt{s} = 200$ GeV from STAR experiment in comparison to the model predictions. Black solid markers are the data points and lines of different colors shows different model predictions.

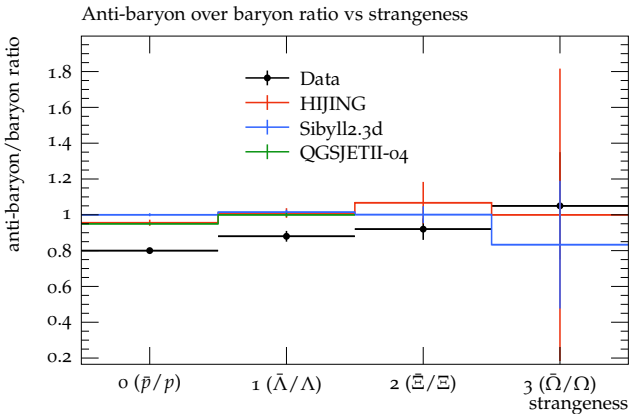


Figure 2: Particles ratio and p_T vs mass at $\sqrt{s} = 200$ GeV

different parton distribution functions for light quark may explain this deviation [38]. On the other hand, the ratio from all models does not show a strong dependence on the strangeness content. This means that the models still need improvements to include the strangeness content. A possible explanation for experimental data as well as the model predictions in fig. 1 and fig. 2 is that the particles are not predominantly produced from the quark-jet fragmentation over the measured p_T range.

In order to understand the model behavior for different particle ratios, a detailed study has been preformed at LHC energies as well. LHCb experiment at the LHC reported the anti-baryon to baryon and baryon to meson ratios as a function of rapidity and p_T in pp collisions at $\sqrt{s} = 0.9$ and 7 TeV [36]. The p_T is divided into various regions; $0.25 < p_T < 0.65$ GeV/c, $0.65 < p_T < 1.0$ GeV/c and $1.0 < p_T < 2.5$ GeV/c in the rapidity $2 < y < 4$ region. The anti-baryon to baryon ($\bar{\Lambda}/\Lambda$) and baryon to meson ($\bar{\Lambda}/K_S^0$) ratios are then compared with different model predictions at the given p_T and y regions.

Figure 3 (left column) shows the model prediction of anti-baryon to baryon ($\bar{\Lambda}/\Lambda$) ratios as a function of rapidity (y) in comparison to the data from LHCb experiment [36]. The y dependence can be seen in the experimental data. It has been observed that at all p_T regions, HIJING and Sibyll model does not show strong rapidity (y) dependence at all and therefore, the ratio is about unity which means that in HIJING and Sibyll, the same number of $\bar{\Lambda}$ are produced as that of Λ . However, the QGSJET model describes the distribution of $\bar{\Lambda}/\Lambda$ ratios reasonably well. At $0.65 < p_T < 1.0$ GeV/c region, below $y < 3$, QGSJET slightly overpredict the experimental results but at

high y region it is in good agreement with the experimental observations. Overall, QGSJET is in good agreement with data at all the p_T regions.

Figure 3 (right column) depict the model prediction of baryon to meson (Λ/K_S^0) ratios as a function of rapidity (y) compared with the experimental results. At all p_T regions, it can be seen that, again the predictions of HIJING and Sibyll shows no strong rapidity (y) dependence. However, HIJING predicts the experimental results reasonably well as compared to the Sibyll and QGSJET. Sibyll completely underpredict the experimental as well as HIJING and QGSJET results at $0.25 < p_T < 0.65$ GeV/c and $0.65 < p_T < 1.0$ GeV/c regions. QGSJET slightly underpredict the experimental data at $0.25 < p_T < 0.65$ GeV/c where gives a reasonable description at $0.65 < p_T < 1.0$ GeV/c region. At $1.0 < p_T < 2.5$ GeV/c, all of the model prediction are roughly similar and are consistent with experimental data.

We have also combined all the p_T regions from $0.25 < p_T < 2.5$ GeV/c and studied the models predictions of various ratios as a function of p_T , rapidity (y) and rapidity loss (Δy) in comparison with experimental results. Figure 4a shows the $\bar{\Lambda}/\Lambda$ ratio as a function of rapidity (y) at all p_T range. Only QGSJET model is consistent with experimental data while HIJING and Sibyll does not show strong rapidity dependence. $\bar{\Lambda}/K_S^0$ ratio as a function of rapidity (y) is shown in fig. 4b. HIJING results are slightly close to the data and does not show rapidity dependence. On the other hand, Sibyll and QGSJET underpredict the experimental data and HIJING data significantly. Figure 4c depict the $\bar{\Lambda}/\Lambda$ ratio as a function of p_T in the rapidity range $2.0 < y < 4.0$. Only QGSJET agrees with the data at $p_T > 0.8$ GeV/c, while HIJING and Sibyll significantly overshoot the data.

HIJING does not show p_T dependence at all while Sibyll and QGSJET does. $\bar{\Lambda}/K_S^0$ ratio as a function of p_T can be seen in fig. 4d. QGSJET and HIJING reasonably describe the data at as well as the ratio distribution at all p_T regions while Sibyll slightly underpredict the data at almost all the p_T regions. Figures 4e and 4f respectively shows the $\bar{\Lambda}/\Lambda$ and $\bar{\Lambda}/K_S^0$ ratios as a function of rapidity loss (Δy). In case of $\bar{\Lambda}/\Lambda$ in fig 4e, only QGSJET describe the data and distribution while HIJING and Sibyll overshoot the data. HIJING also does not shows the Δy dependence at all. $\bar{\Lambda}/K_S^0$ ratios from fig. 4f almost all of the models underpredict the data significantly except HIJING whose predictions are close to the experimental observations.

For the comparison study of various particle ratios in pp collisions at $\sqrt{s} = 7$ TeV, the p_T is divided into various regions; $0.15 < p_T < 0.65$ GeV/c, $0.65 < p_T < 1.0$ GeV/c and $1.0 < p_T < 2.5$ GeV/c in the rapidity $2 < y < 4$ region. The anti-baryon to baryon ($\bar{\Lambda}/\Lambda$) and baryon to meson ($\bar{\Lambda}/K_S^0$) ratios are then compared with different model predictions at the given p_T and y regions.

Figure 5 (left column) shows the model prediction of anti-baryon to baryon ($\bar{\Lambda}/\Lambda$) ratios as a function of rapidity (y) in comparison to the data from LHCb experiment in pp collisions at $\sqrt{s} = 7$ TeV [36]. A slight y dependence can be observed from the experimental measurements. At $0.15 < p_T < 0.65$ GeV/c region, the ratio predictions of the models is close to unity while experimental data lies under the model predictions. At $0.65 < p_T < 1.0$ GeV/c region, Sibyll and QGSJET predictions are close to unity while small deviation is observed in HIJING predictions. The HIJING slightly describe the shape of the ratio distribution. The HIJING model at $1.0 < p_T < 2.5$ GeV/c region behave differently and overshoot the data and hence does not describe the distribution shape correctly. On the other hand, Sibyll and QGSJET ratio is close to unity. Overall, none of the model describe the experimental data and distribution shape accurately at all p_T regions.

Figure 5 (right column) depict the model prediction of baryon to meson ($\bar{\Lambda}/K_S^0$) ratios as a function of rapidity (y) compared with the experimental results. At $0.15 < p_T < 0.65$ GeV/c region, HIJING and QGSJET describe the experimental data within uncertainties, however Sibyll completely fail to predict the experimental results and hence underpredict the data. At $0.65 < p_T < 1.0$ GeV/c region, QGSJET predictions matches with data within uncertainties while HIJING slightly undershoot the data. Sibyll again, completely fail to predict the experimental results and hence undershoot the experimental observations and both models. At $1.0 < p_T < 2.5$ GeV/c region, Sibyll predictions are slightly closer to the HIJING but still lower than HIJING and QGSJET predictions and hence experimental data. Only QGSJET model completely describe the experimental observations completely.

Figure 6a shows the $\bar{\Lambda}/\Lambda$ ratio as a function of rapidity (y) at all p_T range from $0.15 < p_T < 2.50$ GeV/c region. All the model predictions are close to unity and roughly about same while data lies below the model predictions and shows the decreasing trend with rapidity y . All the models does not shows rapidity dependence at all. The $\bar{\Lambda}/K_S^0$ ratio as a function of rapidity (y) is shown in fig. 6b. Only the prediction of QGSJET is in good agreement

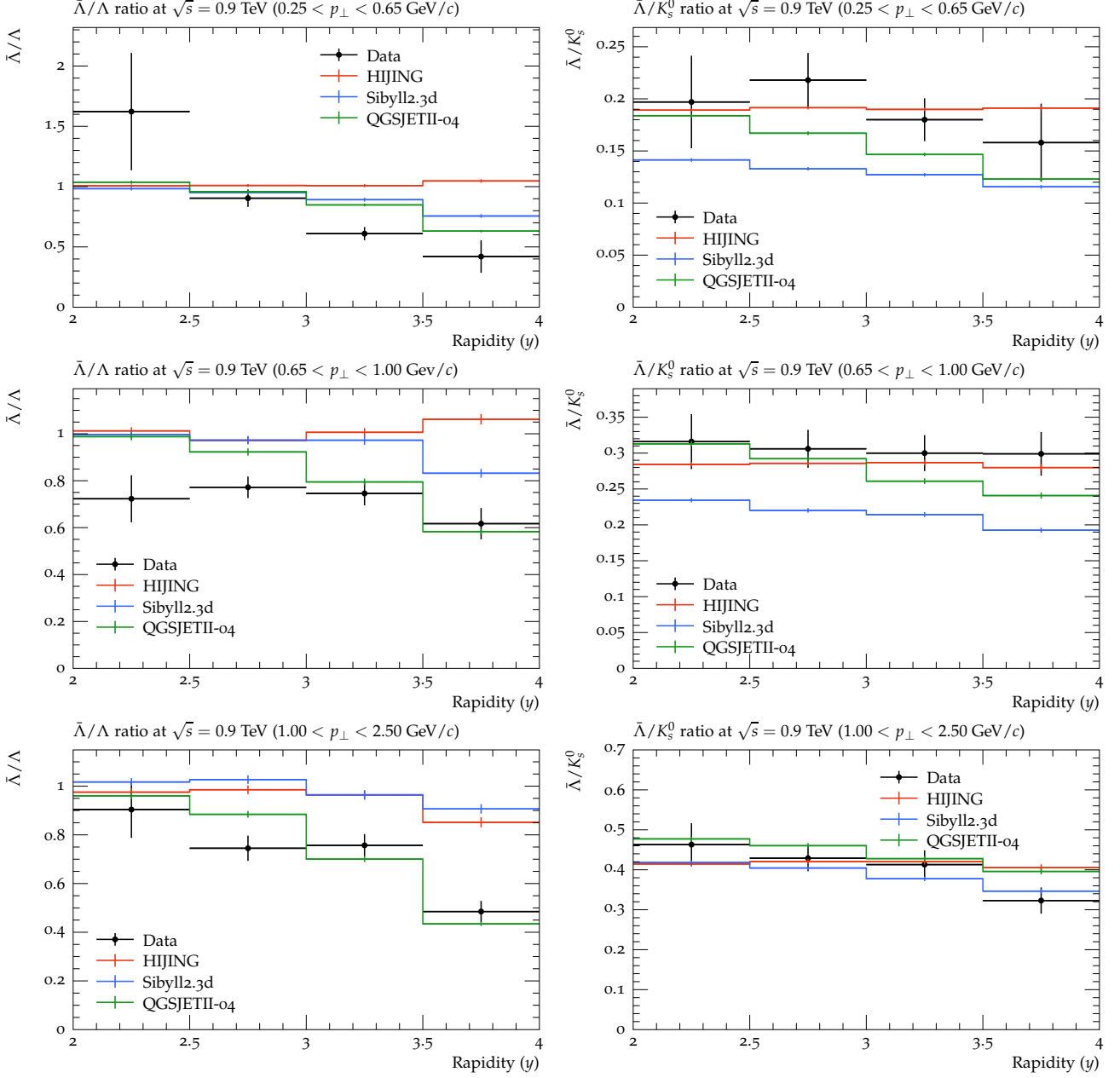


Figure 3: (Left column) anti-baryon to baryon ($\bar{\Lambda}/\Lambda$) ratios as a function of rapidity (y) (Right Column) anti-baryon to meson ($\bar{\Lambda}/K_s^0$) ratios in pp collisions $\sqrt{s} = 0.9$ TeV at different p_T regions. Black solid markers are the data points and lines of different colors shows different model predictions.

with data while HIJING and Sibyll predictions are undershooting the data and QGSJET significantly. Figure 6c depict the $\bar{\Lambda}/\Lambda$ ratio as a function of p_T in the rapidity range $2.0 < y < 4.0$. None of the model describe the experimental data. The model predictions are close to unity while data lies below around 0.95. Both data and all the models does not show p_T dependence. $\bar{\Lambda}/K_s^0$ ratio as a function of p_T can be seen in fig. 6d. QGSJET and HIJING reasonably describe the data at within uncertainties as well as the ratio distribution at all p_T regions while Sibyll slightly underpredict the data at almost all the p_T regions. Figures 6e and 6f respectively shows the $\bar{\Lambda}/\Lambda$ and $\bar{\Lambda}/K_s^0$ ratios as a function of rapidity loss (Δy). In case of $\bar{\Lambda}/\Lambda$ in fig 4e, all of the model predictions are close to unity and data lies significantly lower to the model data. None of the model explains this distribution well. $\bar{\Lambda}/K_s^0$ ratios from fig. 6a almost all of the models underpredict the data significantly except QGSJET whose

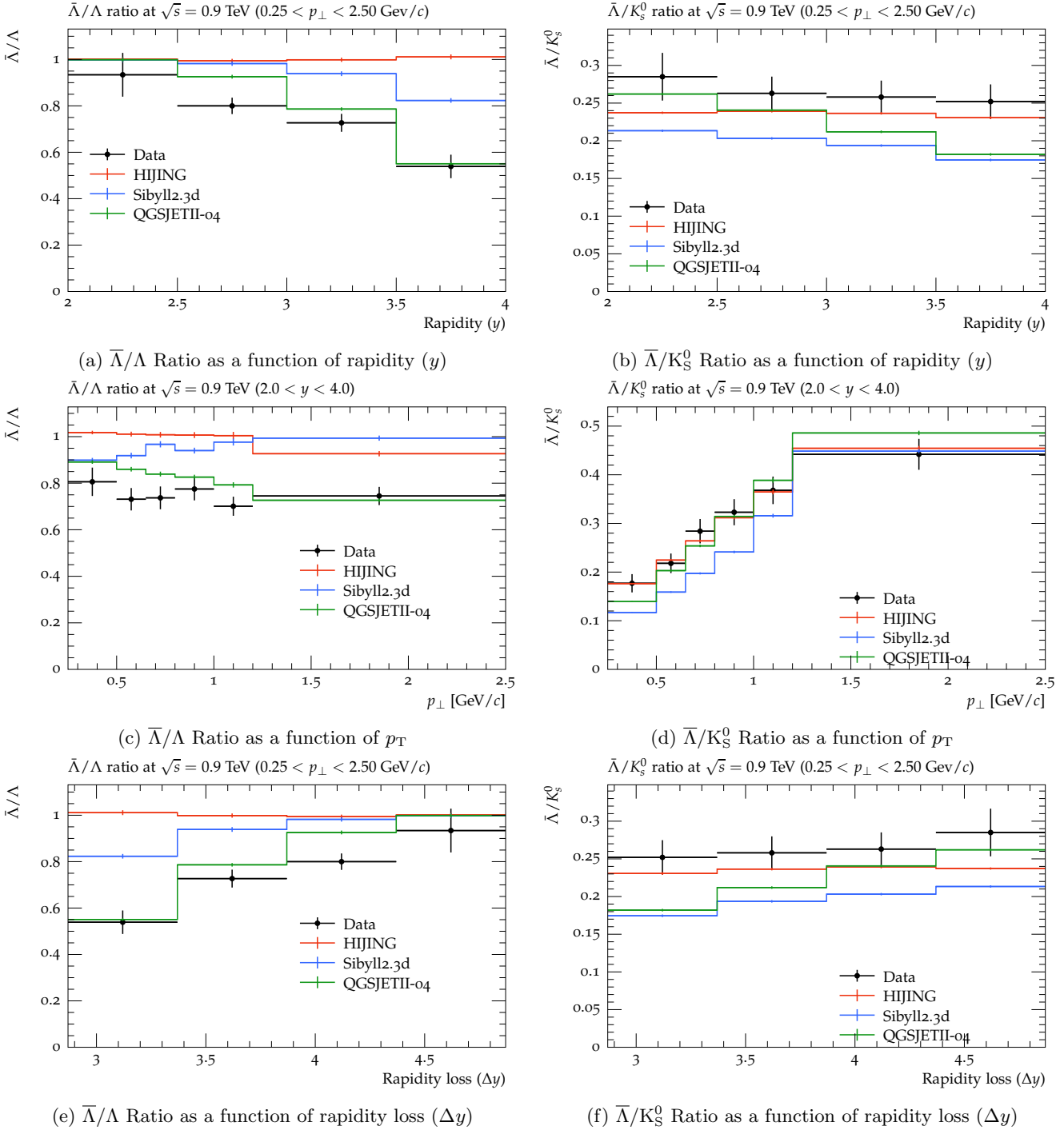


Figure 4: Different ratios as a function of p_T , rapidity (y) and rapidity loss (Δy) in pp collisions at $\sqrt{s} = 0.9$ TeV from LHCb experiment in comparison to the model predictions. Black solid markers are the data points and lines of different colors shows different model predictions.

predictions are consistent with the experimental observations.

Figure 7a shows the Λ/K_s^0 ratio as a function of p_T from pp collisions at $\sqrt{s} = 7$ TeV in comparison with the experimental results. The data is observed to show no rapidity y dependence and almost follows the straight line. It can also be seen that all of the models also do not show the rapidity y dependence at all, but QGSJET is the only model which predicts the same results as that of data within uncertainties. Sibyll and HIJING predictions

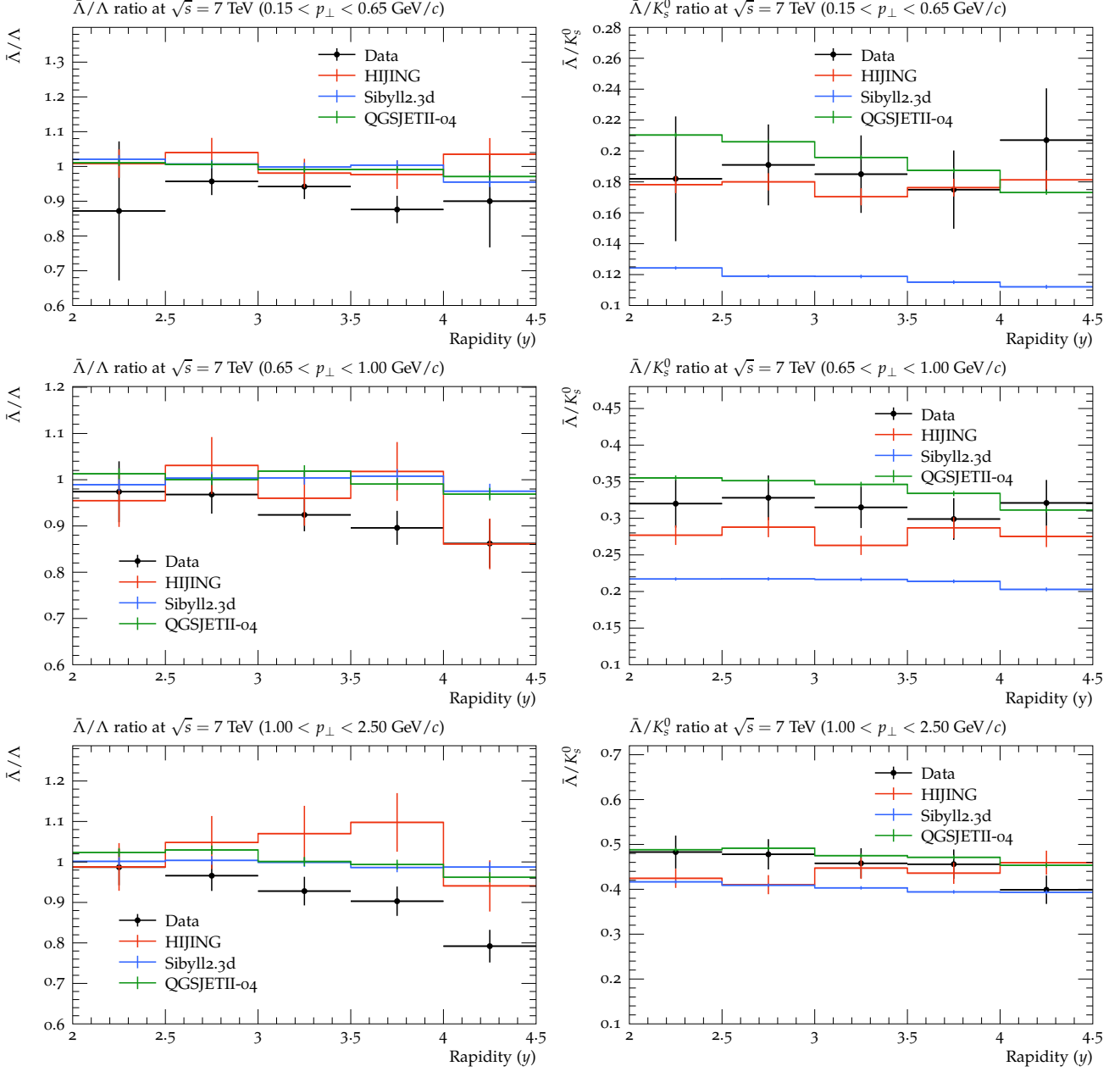


Figure 5: (Left column) anti-baryon to baryon ($\bar{\Lambda}/\Lambda$) ratios as a function of rapidity (y) (Right Column) anti-baryon to meson ($\bar{\Lambda}/K_s^0$) ratios in pp collisions $\sqrt{s} = 7$ TeV at different p_T regions. Black solid markers are the data points and lines of different colors shows different model predictions.

are very close to each other but underpredict the experimental data as well as QGSJET roughly by 15% and 10% respectively. Figure 7b presents the Λ/K_s^0 ratio as a function of p_T . It is observed that there is sharper increases in Λ spectrum with the increase in low p_T ($p_T < 1.5$ GeV/ c) and Λ production is relatively larger at the intermediate p_T region ($1.5 \leq p_T \leq 4.0$ GeV/ c). The same shape difference between Λ and K_s^0 can be seen as reported in baryon to meson ratios [39]. HIJING is observed to predict almost similar shape and experimental results from low to intermediate p_T regions, i.e., upto $p_T \leq 2.5$ GeV/ c . Sibyll slightly underpredict the data upto $p_T < 1.5$ GeV/ c and overshoot at higher p_T regions. QGSJET on the other hand slightly overpredict the experimental and both model data upto $p_T < 1.5$ GeV/ c and undershoot at above p_T regions. This difference in the shape in experimental results as well as model predictions may be related to fact that there is significant contribution from

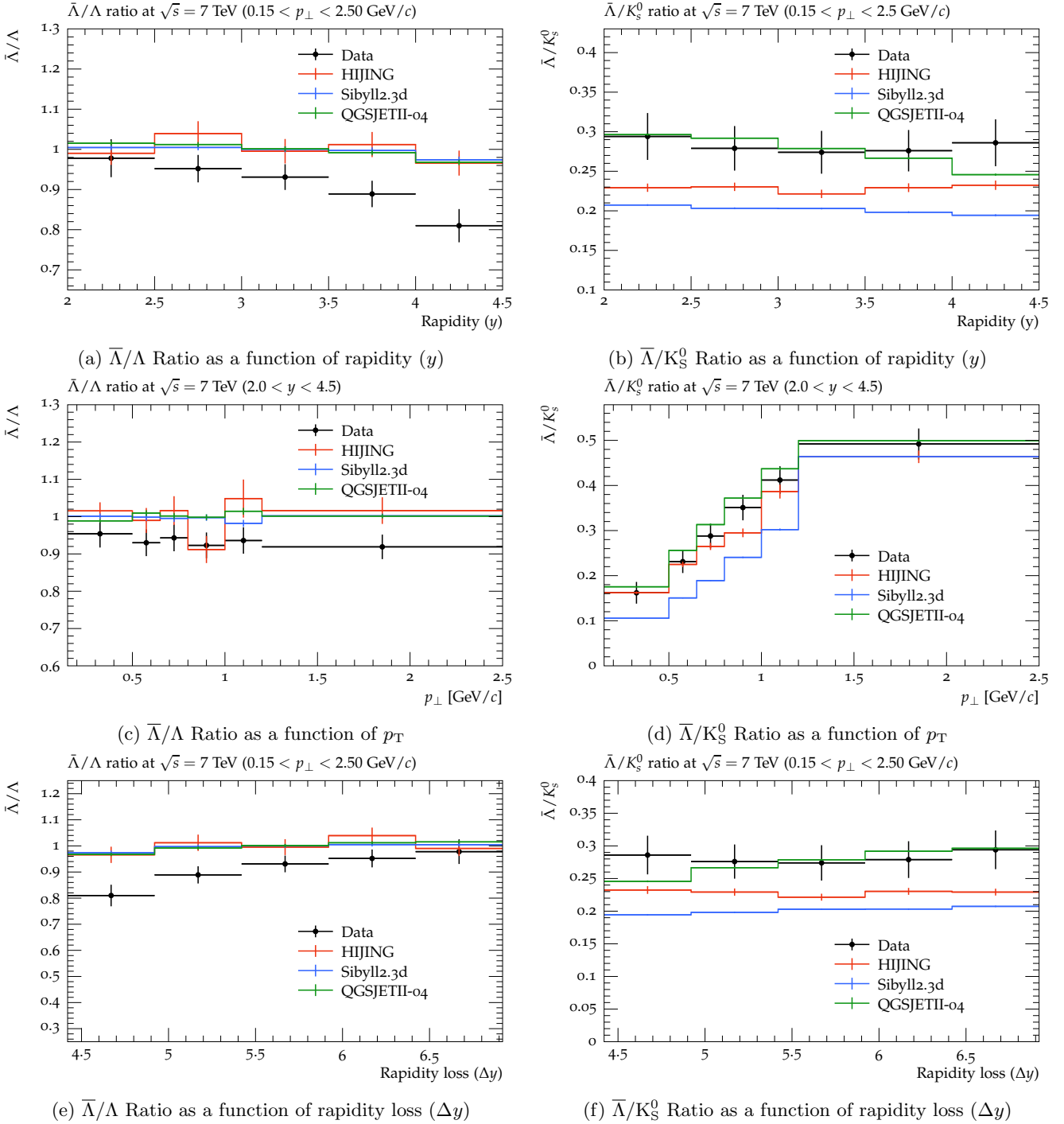


Figure 6: Different ratios as a function of p_T , rapidity (y) and rapidity loss (Δy) in pp collisions at $\sqrt{s} = 7$ TeV from LHCb experiment in comparison to the model predictions. Black solid markers are the data points and lines of different colors shows different model predictions.

the fragmentation processes to meson production as compared to the baryon production which is based on mass and energy arguments. Furthermore, the measurements of Ξ^-/Λ ratios has also been preformed with these models. Figure 7c shows the Ξ^-/Λ ratio as a function of rapidity y . The QGSJET model does not include the definition of Ξ particle therefore no comparison can be made. However, Hijing and Sibyll predicts almost similar results in comparison to the experimental data within uncertainties. Figure 7d presents Ξ^-/Λ ratios as a function of p_T .

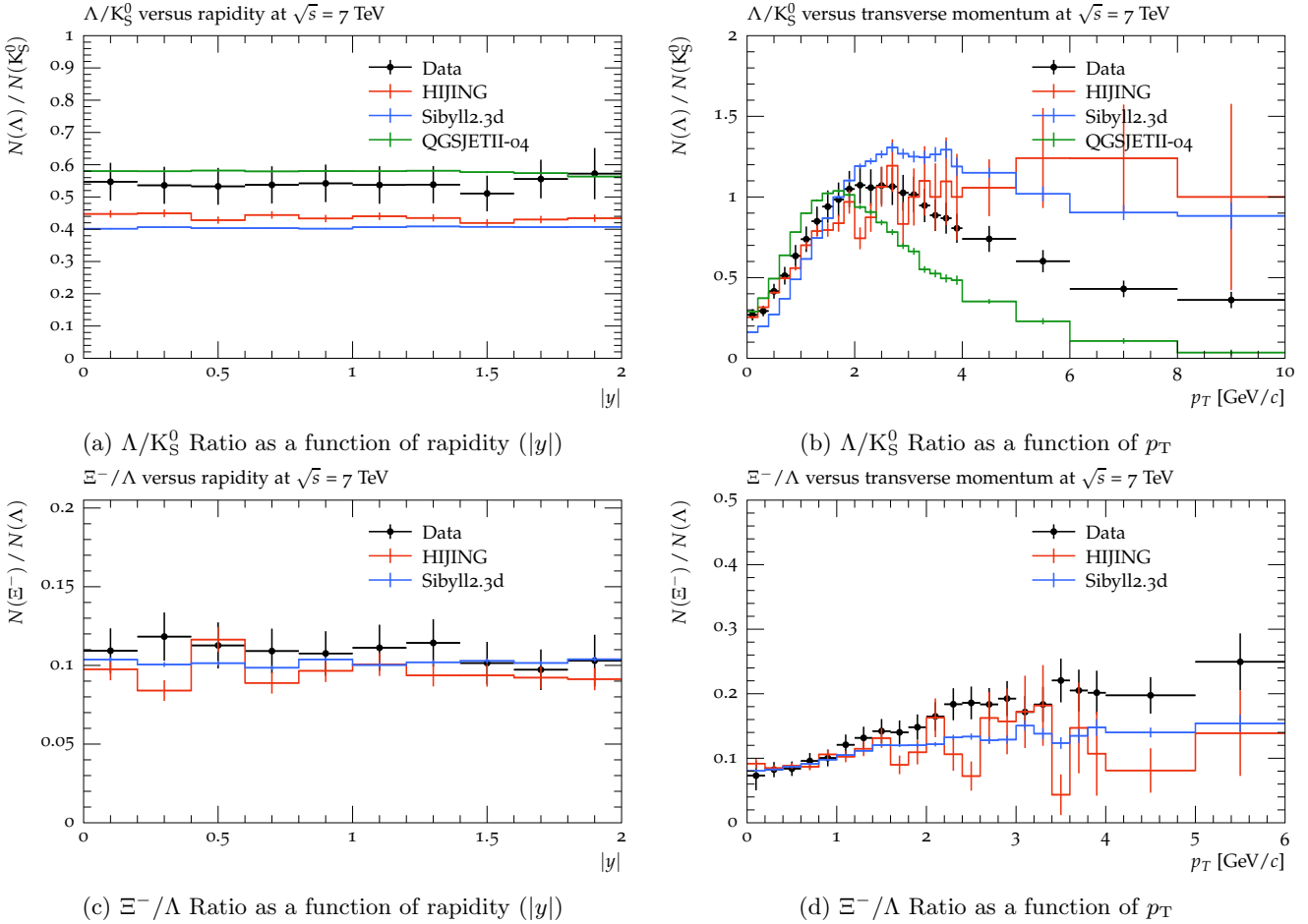


Figure 7: Different ratios as a function of p_T and rapidity (y) in pp collisions at $\sqrt{s} = 7$ TeV from LHCb experiment in comparison to the model predictions. Black solid markers are the data points and lines of different colors shows different model predictions.

Both models Sibyll and HIJING describe the data upto $p_T < 1.5$ GeV/c, while underpredict the data at higher p_T regions. Sibyll shows flat distribution at higher p_T regions while fluctuation is observed in HIJING predictions which may be due to statistics. For a quantitative description of the particles' ratio, we have calculated the values of χ^2/n for all models for the aforementioned energies. The Values are tabulated in Table 1, where the first column shows the energy followed by the figures and particles ratios in column 2 and 3 respectively. The following three columns show the values of the χ^2/n for the HIJING, Sibyll2.3d and QGSJETII-04 models respectively. The last column shows the values of n , where n shows the number of measured points on x-axis in each case. Taking into account the statistical error bars in the models' prediction and the values of the χ^2/n for Fig. 1, it is clear that the models are in good agreement with the experimental data while large values of χ^2/n for Fig. 2 show that models failed to reproduce the measurements. At 0.9 and 7 TeV, the QGSJET model has consistently the lowest values of χ^2/n as compared to the other two models. For different particle ratios ($\bar{\Lambda}/K_S^0$, Ξ^-/Λ) the HIJING model performed better even than the QGSJET model but failed completely to prediction the same particles ratio ($\bar{\Lambda}/\Lambda$) at 0.9 and 7 TeV. The values of χ^2/n for the different particles' ratios in the Sibyll model are lower than the HIJING but comparatively higher than the QGSJET model but have very high values for the same particles' ratios.

Table 1. The values of the χ^2/n for the HIJING, Sibyll2.3d and QGSJETII-04 models at $\sqrt{s} = 0.2, 0.9$ and 7 TeV.

Energy	Figure	ratio	χ^2/n	χ^2/n	χ^2/n	n
			HIJING	Sibyll2.3d	QGSJETII - 04	
200 GeV	1(a)	$\bar{\Lambda}/\Lambda$ vs p_T	2.29	1.78	1.99	21
	1(b)	$\bar{\Xi}^+/\Xi^-$ vs p_T	0.99	0.71	-	11
	2	\bar{B}/B vs strangeness	18.75	63.23	75.76	4
900 GeV	3(a)	$\bar{\Lambda}/\Lambda$ vs y	18.86	8.19	5.62	4
	3(b)	$\bar{\Lambda}/K_S^0$ vs y	0.52	5.00	1.85	4
	3(c)	$\bar{\Lambda}/\Lambda$ vs y	22.10	12.72	4.40	4
	3(d)	$\bar{\Lambda}/K_S^0$ vs y	0.48	9.62	1.56	4
	3(e)	$\bar{\Lambda}/\Lambda$ vs y	23.43	30.52	2.41	4
	3(f)	$\bar{\Lambda}/K_S^0$ vs y	1.70	0.67	1.45	4
900 GeV	4(a)	$\bar{\Lambda}/\Lambda$ vs y	39.88	20.92	3.70	4
	4(b)	$\bar{\Lambda}/K_S^0$ vs y	1.32	8.12	3.83	6
	4(c)	$\bar{\Lambda}/\Lambda$ vs p_T	26.88	20.81	3.14	6
	4(d)	$\bar{\Lambda}/K_S^0$ vs p_T	0.18	7.22	1.41	6
	4(e)	$\bar{\Lambda}/\Lambda$ vs Δy	39.88	20.92	3.70	4
	4(f)	$\bar{\Lambda}/K_S^0$ vs Δy	1.32	8.12	3.83	4
7000 GeV	5(a)	$\bar{\Lambda}/\Lambda$ vs y	1.40	2.74	2.41	5
	5(b)	$\bar{\Lambda}/K_S^0$ vs y	0.21	6.03	0.45	5
	5(c)	$\bar{\Lambda}/\Lambda$ vs y	0.76	3.43	3.39	5
	5(d)	$\bar{\Lambda}/K_S^0$ vs y	1.52	11.58	0.90	5
	5(e)	$\bar{\Lambda}/\Lambda$ vs y	2.86	6.17	5.81	5
	5(f)	$\bar{\Lambda}/K_S^0$ vs y	1.44	2.71	0.71	5
7000 GeV	6(a)	$\bar{\Lambda}/\Lambda$ vs y	4.44	6.48	6.36	5
	6(b)	$\bar{\Lambda}/K_S^0$ vs y	3.47	8.20	0.44	5
	6(c)	$\bar{\Lambda}/\Lambda$ vs p_T	2.13	3.19	3.89	6
	6(d)	$\bar{\Lambda}/K_S^0$ vs p_T	0.90	9.60	0.57	6
	6(e)	$\bar{\Lambda}/\Lambda$ vs Δy	4.44	6.48	6.36	5
	6(f)	$\bar{\Lambda}/K_S^0$ vs Δy	3.47	8.20	0.44	5
7000 GeV	7(a)	Λ/K_S^0 vs $ y $	2.97	5.17	0.52	10
	7(b)	Λ/K_S^0 vs p_T	1.29	9.67	9.66	24
	7(c)	Ξ^-/Λ vs $ y $	0.97	0.47	-	10
	7(d)	Ξ^-/Λ vs p_T	2.36	2.47	-	22

4 Conclusion

We have performed systematic study of different particle ratios $\bar{\Lambda}/\Lambda$, $\bar{\Lambda}/K_S^0$ and Ξ^-/Λ as a function of rapidity y and p_T from pp collisions at $\sqrt{s} = 0.2, 0.9$, and 7 TeV using Sibyll, HIJING and QGSJET and detailed comparison has been made with available experimental data. The anti-baryon to baryon ($\bar{\Lambda}/\Lambda$) ratio is considered as the measure of baryon transport number in pp collisions to final state hadrons. It has been observed from the model comparison that, none of the single model completely predict the experimental observations completely. However, QGSJET model predictions are close to the experimental results in case of ratios as a function of rapidity y . HIJING on the other hand is in good agreement with $\bar{\Lambda}/K_S^0$ ratios as a function of p_T .

The $\bar{\Lambda}/K_S^0$ ratios as a function of p_T shows the increasing trend at $\sqrt{s} = 0.9$, and 7 TeV suggest that in data, more baryons are expected to produce compared to mesons in strange hadronisation specifically at high p_T regions. HIJING and QGSJET models generally support the experimental data as well as the above statement, however, Sibyll does not. Further improvement is required in order to fully understand the strange hadron production mechanisms particularly at low p_T regions. These ratios are then further studied as a function of rapidity loss (Δy), all of the models fails to produce the experimental results well. In fact, it is seen that models are somehow independent of rapidity.

A current study of V^0 production ratios using various pQCD based models and cosmic-ray air shower based MC generators will be helpful for the development and hence, further improve the predictions of Standard Model physics at RHIC and LHC experiments and it may also be helpful for defining the baseline for new discoveries.

References

- [1] H. Yassin, E. R. A. Elyazeed and A. N. Tawfik, Phys. Scripta **95**, no.7, 7 (2020) doi:10.1088/1402-4896/ab9128 [arXiv:1912.01404 [hep-ph]].
- [2] Muhammad Waqas and Guangxiong Peng and Fu-Hu Liu J. Phys. G: Nucl. Part. Phys. **48** 075108 (2021) doi:10.1088/1361-6471/abdd8d
- [3] Waqas, Muhammad, Liu, Fu-Hu, Wang, Rui-Qin and Siddique, Irfan, The European Physical Journal A **56**, 188 (2020) doi:10.1140/epja/s10050-020-00192-y
- [4] M. M. Aggarwal *et al.* [STAR], Phys. Rev. C **83**, 024901 (2011) doi:10.1103/PhysRevC.83.024901 [arXiv:1010.0142 [nucl-ex]].
- [5] J. Adam *et al.* [ALICE], Nature Phys. **13**, 535-539 (2017) doi:10.1038/nphys4111 [arXiv:1606.07424 [nucl-ex]].
- [6] J. Adam *et al.* [ALICE], Phys. Lett. B **753**, 319-329 (2016) doi:10.1016/j.physletb.2015.12.030 [arXiv:1509.08734 [nucl-ex]].
- [7] V. Khachatryan *et al.* [CMS], JHEP **09**, 091 (2010) doi:10.1007/JHEP09(2010)091 [arXiv:1009.4122 [hep-ex]].
- [8] V. Khachatryan *et al.* [CMS], Phys. Lett. B **765**, 193-220 (2017) doi:10.1016/j.physletb.2016.12.009 [arXiv:1606.06198 [nucl-ex]].
- [9] J. Adam *et al.* [ALICE], Nature Phys. **13**, 535-539 (2017) doi:10.1038/nphys4111 [arXiv:1606.07424 [nucl-ex]].
- [10] E. Abbas *et al.* [ALICE], Eur. Phys. J. C **73**, 2496 (2013) doi:10.1140/epjc/s10052-013-2496-5 [arXiv:1305.1562 [nucl-ex]].
- [11] A. E. M. Billmeier [STAR], J. Phys. G **30**, S363-S368 (2004) doi:10.1088/0954-3899/30/1/043
- [12] D. Colella [ALICE], Int. J. Mod. Phys. Conf. Ser. **46**, 1860017 (2018) doi:10.1142/S2010194518600170
- [13] R. Aaij *et al.* [LHCb], JHEP **08**, 034 (2011) doi:10.1007/JHEP08(2011)034 [arXiv:1107.0882 [hep-ex]].
- [14] Muhammad Ajaz et al., Results in Physics **30**, 104790 (2021) doi:10.1016/j.rinp.2021.104790
- [15] M. Ajaz, M. Waqas, G. X Peng et al. Eur. Phys. J. Plus **137**, 52 (2022). doi:10.1140/epjp/s13360-021-02271-5 [arXiv:2112.03187 [hep-ph]]
- [16] S. Ullah, M. Ajaz, Z. Wazir, et al. Sci Rep, **9**, 11811 (2019) doi:10.1038/s41598-019-48272-4
- [17] M. Ajaz, S. Ullah, Y. Ali, and H. Younis. Modern Physics Letters A, **33**, 1850038 (2018) doi:10.1142/S0217732318500384
- [18] David d'Enterria, Ralph Engel, Tanguy Pierog, Sergey Ostapchenko, and Klaus Werner. Astroparticle Physics, **35** 98–113 (2011) doi:10.1016/j.astropartphys.2011.05.002
- [19] S. Ullah, Y. Ali, M. Ajaz, U. Tabassam, and Q. Ali. International Journal of Modern Physics A, **33**, 1850108 (2018) doi:10.1142/S0217751X18501087
- [20] Muhammad Ajaz, M. Tufail, and Y. Ali. Arabian Journal for Science and Engineering, **45**, 411–416 (2019)
- [21] S. Ullah, M. Ajaz, and Y. Ali. EPL, **123**, 31001 (2018) doi:10.1209/0295-5075/123/31001
- [22] M. Ajaz, M. Bilal, Y. Ali, M. K. Suleymanov, and K. H. Khan. Modern Physics Letters A, **34**, 1950090 (2019) doi:10.1142/S0217732319500901

[23] Muhammad Ajaz, Ahmed M. Khubrani, Muhammad Waqas, Abd Al Karim Haj Ismail, Elmuez A. Dawi, Collective properties of hadrons in comparison of models prediction in pp collisions at 7 TeV, Results in Physics, **36**, 105433 (2022) doi:10.1016/j.rinp.2022.105433.

[24] Pei-Pin Yang, Muhammad Ajaz, Muhammad Waqas, Fu-Hu Liu, and Mais Suleymanov. Journal of Physics G: Nuclear and Particle Physics, **49**, 055110 (2022) doi:10.1088/1361-6471/ac5d0b

[25] M.H.M. Soleiman, Arab J. Nucl. Sci. Appl., Vol. **53**, 1, 46-57 (2020) doi: 10.21608/ajnsa.2019.9617.1182

[26] M. Gyulassy and X. N. Wang, Comput. Phys. Commun. **83**, 307 (1994) doi:10.1016/0010-4655(94)90057-4 [arXiv:nucl-th/9502021 [nucl-th]].

[27] X. N. Wang and M. Gyulassy, Phys. Rev. D **45**, 844-856 (1992) doi:10.1103/PhysRevD.45.844

[28] X. N. Wang and M. Gyulassy, Phys. Rev. D **44**, 3501-3516 (1991) doi:10.1103/PhysRevD.44.3501

[29] D. Kieda, M. Salamon and B. Dingus, Proceedings, 26th International Cosmic Ray Conference (ICRC) : Contributed Papers: Salt Lake City, USA, August 17-25, 1999,

[30] F. Riehn, R. Engel, A. Fedynitch, T. K. Gaisser and T. Stanev, Phys. Rev. D **102**, no.6, 063002 (2020) doi:10.1103/PhysRevD.102.063002 [arXiv:1912.03300 [hep-ph]].

[31] F. Riehn, H. P. Dembinski, R. Engel, A. Fedynitch, T. K. Gaisser and T. Stanev, PoS **ICRC2017**, 301 (2018) doi:10.22323/1.301.0301 [arXiv:1709.07227 [hep-ph]].

[32] S. Ostapchenko, Nucl. Phys. B Proc. Suppl. **151**, 143-146 (2006) doi: 10.1016/j.nuclphysbps.2005.07.026 [arXiv:hep-ph/0412332 [hep-ph]].

[33] S. Ullah, M. Ajaz and Y. Ali, EPL **123**, no.3, 31001 (2018) doi: 10.1209/0295-5075/123/31001

[34] M. Ajaz et al., Modern Physics Letters A **34**, 1950090 (2019) doi: 10.1142/S0217732319500901

[35] B. I. Abelev *et al.* [STAR], Phys. Rev. C **75**, 064901 (2007) doi:10.1103/PhysRevC.75.064901 [arXiv:nucl-ex/0607033 [nucl-ex]].

[36] R. Aaij *et al.* [LHCb], JHEP **08**, 034 (2011) doi:10.1007/JHEP08(2011)034 [arXiv:1107.0882 [hep-ex]].

[37] X. N. Wang, Phys. Rev. C **58**, 2321 (1998) doi:10.1103/PhysRevC.58.2321 [arXiv:hep-ph/9804357 [hep-ph]].

[38] A. D. Martin, W. J. Stirling and R. G. Roberts, Phys. Rev. D **50**, 6734-6752 (1994) doi:10.1103/PhysRevD.50.6734 [arXiv:hep-ph/9406315 [hep-ph]].

[39] J. Adams *et al.* [STAR], Phys. Lett. B **637**, 161-169 (2006) doi:10.1016/j.physletb.2006.04.032 [arXiv:nucl-ex/0601033 [nucl-ex]].